Topology and Spin Alignment in a Novel Organic High-Spin Molecule, 3,4′-Bis(phenylmethylene)biphenyl, As Studied by ESR and a Generalized UHF Hubbard Calculation

Yoshio Teki,† Ikuo Fujita, Takeji Takui, Takamasa Kinoshita, and Koichi Itoh*,†

Contribution from the Department of Chemistry, Faculty of Science, Osaka City University, 3-3-138 Sugimoto, Sumiyoshi-ku, Osaka 558, Japan

Received June 13, 1994®

Abstract: In order to examine the role of π topology in spin alignment of organic molecules, a novel high-spin hydrocarbon, 3,4′-bis(phenylmethylene)biphenyl, has been designed, synthesized, and characterized by powder-pattern and single-crystal ESR spectroscopies. The spin multiplicity of its electronic ground state is a quintet ($S = 2$) in contrast to its π-topological isomer, 3,3′-bis(phenylmethylene)biphenyl (ground-state singlet). The g and fine-structure tensors have been determined accurately: $g = 2.003$ (isotropic), $D = 0.1250$ cm^{-1}, and $E = -0.0065$ cm^{-1}. The striking contrast in spin multiplicity clearly shows that spin alignment in organic molecules is highly dependent on the topology in their π electron networks. This electronic structure has been clarified by an unrestricted Hartree−Fock calculation using a generalized Hubbard model, demonstrating that this approach is useful for large quantum systems such as organic high-spin hydrocarbons. The mechanism of the intramolecular spin alignment in this molecule has been discussed with the help of the theoretical calculation. The most probable molecular conformation of this high-spin molecule in benzophenone host crystals has been derived from the observed fine-structure tensor as compared with those calculated semiempirically.

I. Introduction

In recent years, organic/molecular based magnetism has attracted continuing interest in chemistry and the related fields.[1,2] Organic high-spin molecules have been involved as one of the most suitable model compounds in many important developments in research on purely organic ferromagnetic materials and ferromagnetic polymers.[3,4] High-spin molecules are also important for the study of spin alignment in organic molecules.[5−18] We define π-topological isomers as high-spin molecules which differ from others only in topology in the π electron network owing to the different linking positions of their π-bonds. Our extensive studies[7,9,10,12−14,17] have shown that the electronic structures of the π-topological isomers are characterized by the existence of the low-lying excited states with spin multiplicities higher than those of the ground states. *a,a′*-Bis(phenylmethylene)biphenyl shown below is one example. Molecule **2** is a π-topological isomer of molecule **1**. The salient features of the electronic states of the high-spin carbenes arise from the strong spin correlation among the delocalized π electrons and the localized "n" electrons at the divalent carbon atoms. The behavior of correlated electron spins in high-spin carbenes and other organic high-spin molecules reported by several authors[5b,19−30] is of key importance in rationalizing organic

† Present address: Department of Material Science, Faculty of Science, Osaka City University, 3-3-138 Sugimoto, Sumiyoshi-ku, Osaka 558, Japan.

® Abstract published in *Advance ACS Abstracts*, November 1, 1994.

(1) For a recent overview, see: Miller, J. S.; Dougherty, D. A., Eds. *Mol. Cryst. Liq. Cryst.* **1989**, *176*, 1−562. *Advanced Organic Solid State Materials*; Chiang, L. Y., Chaikin, P. M., Cowan, D. O., Eds.; Materials Research Society: Pittsburgh, PA, 1989; pp 3−92. *Molecular Magnetic Materials*; Gatteschi, D., Kahn, O., Miller, J. S., Palacio, F., Eds.; Kluwer Academic: Dordrecht, 1991; Vol. A198. Iwamura, H.; Miller, J. S., Eds. *Mol. Cryst. Liq. Cryst.* **1993**, *232/233*, 1−360/1−366.

(2) In addition to the two approaches for organic/molecular magnetism, i.e., the charge-transfer interaction approach and the π-topological degeneracy approach, a polaronic ferromagnet approach has recently appeared from both theoretical and experimental sides. See: (a) Fukutome, H.; Takahashi, A.; Ozaki, M. *Chem. Phys. Lett.* **1987**, *133*, 34−38. (b) Kaisaki, D. A.; Chang, W.; Dougherty, D. A. *J. Am. Chem. Soc.* **1991**, *113*, 2764−2766. Dougherty, D. A. *Acc. Chem. Res.* **1991**, *24*, 88−94.

(3) (a) Morimoto, S.; Itoh, K.; Tanaka, F.; Mataga, N. *Preprints of the Symposium on Molecular Structure (Tokyo)* **1968**, 76−77. (b) Mataga, N. *Theor. Chim. Acta* **1968**, *10*, 372−376. (c) Itoh, K. *Bussei* **1971**, *12*, 635−646.

(4) (a) Ovchinnikov, A. A. *Theor. Chim. Acta* **1978**, *47*, 297−304. (b) Klein, D. J.; Nelin, C. J.; Alexander, S.; Matsen, F. A. *J. Chem. Phys.* **1982**, *77*, 3101−3108. (c) Ivanov, C. I.; Tyutyulkov, N.; Olbvich, G.; Brenzen, H.; Polansky, O. E. *Theor. Chim. Acta* **1988**, *73*, 27−42, and references therein. (d) Nasu, K. *Phys. Rev.* **1986**, *B33*, 330−338. (e) Yamaguchi, K.; Toyoda, Y.; Fueno, T. *Synth. Met.* **1987**, *19*, 81−86.

(5) (a) Itoh, K. *Chem. Phys. Lett.* **1967**, *1*, 235−238. (b) Wasserman, E.; Murray, R. E.; Yager, W. A.; Trozzolo, A. M.; Smolinsky, G. *J. Am. Chem. Soc.* **1967**, *89*, 5076−5078.

(6) Takui, T.; Itoh, K. *Chem. Phys. Lett.* **1973**, *19*, 120−124.

(7) Itoh, K. *Pure Appl. Chem.* **1978**, *50*, 1251−1259.

(8) (a) Teki, Y.; Takui, T.; Itoh, K.; Iwamura, H.; Kobayashi, K. *J. Am. Chem. Soc.* **1983**, *105*, 3722−3723. (b) Teki, Y.; Takui, T.; Yagi, H.; Itoh, K.; Iwamura, H. *J. Chem. Phys.* **1985**, *83*, 539−547. (c) Teki, Y.; Takui, T.; Itoh, K.; Iwamura, H.; Kobayashi, K. *J. Am. Chem. Soc.* **1986**, *108*, 2147−2156. (d) Sugawara, T.; Bandow, S.; Kimura, K.; Iwamura, H.; Itoh, K. *J. Am. Chem. Soc.* **1986**, *108*, 368−371.

(9) Teki, Y.; Takui, T.; Kinoshita, T.; Ichikawa, S.; Yagi, H.; Itoh, K. *Chem. Phys. Lett.* **1987**, *141*, 201−205.

(10) Teki, Y.; Takui, T.; Kitano, M.; Itoh, K. *Chem. Phys. Lett.* **1987**, *142*, 181−186.

(11) Teki, Y.; Takui, T.; Itoh, K. *J. Chem. Phys.* **1988**, *88*, 6134−6145.

(12) Itoh, K.; Takui, T.; Teki, Y.; Kinoshita, T. *J. Mol. Electron.* **1988**, *4*, 181−186.

(13) Itoh, K.; Takui, T.; Teki, Y.; Kinoshita, T. *Mol. Cryst. Liq. Cryst.* **1989**, *176*, 49−65.

(14) Takui, T.; Kita, S.; Ichikawa, S.; Teki, Y.; Kinoshita, T.; Itoh, K. *Mol. Cryst. Liq. Cryst.* **1989**, *176*, 67−76.

(15) (a) Fujita, I.; Teki, Y.; Takui, T.; Kinoshita, T.; Itoh, K.; Miko, F.; Sawaki, Y.; Iwamura, H.; Izuoka, A.; Sugawara, T. *J. Am. Chem. Soc.* **1990**, *112*, 4074−4075. (b) Furukawa, K.; Kinoshita, T.; Matsumura, T.; Teki, Y.; Takui, T.; Itoh, K., submitted for publication.

(16) Matushita, M.; Momose, T.; Shida, T.; Teki, Y.; Takui, T.; Itoh, K. *J. Am. Chem. Soc.* **1990**, *112*, 4701−4702.

(17) (a) Okamoto, M.; Teki, Y.; Takui, T.; Kinoshita, T.; Itoh, K. *Chem. Phys. Lett.* **1990**, *173*, 265−270. (b) Teki, Y.; Okamoto, M.; Takui, T.; Kinoshita, T.; Itoh, K., to be submitted for publication.

(18) Sato, K.; Teki, Y.; Takui, T.; Kinoshita, T.; Itoh, K., submitted for publication.

(19) Wasserman, E.; Schueller, K.; Yager, W. A. *Chem. Phys. Lett.* **1968**, *2*, 259−260.

(20) Brickmann, J.; Kothe, G. *J. Chem. Phys.* **1973**, *9*, 2807−2814.

0002-7863/94/1516-11499$04.50/0

magnetism and in generalizing topological classification for open-shell molecules.

In this work, we have studied the ground state of a high-spin hydrocarbon, 3,4′-bis(phenylmethylene)biphenyl (quintet ground state), **1**, whose π-topological isomer is 3,3′-bis(phenylmethylene)biphenyl (singlet ground state), **2**.[7,17]

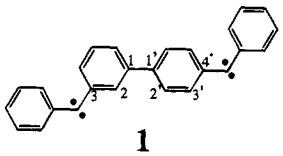

1

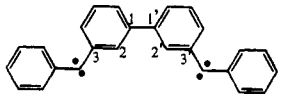

2

As proposed earlier by one of the authors (K.I.),[3,7] Longuet-Higgins' theory[31a] coupled to Hund's rule predicts that a ground-state spin quantum number S^{π}_{MO} of an alternant hydrocarbon is given by

$$S^{\pi}_{MO} = (1/2)(N - 2T) \quad (1)$$

where N is the number of carbon atoms and T is the maximum number of double bonds in the alternant hydrocarbon. On the other hand, the spin prediction theory on the basis of the simple valence bond (VB) picture[4a] gives

$$S^{\pi}_{VB} = (1/2)|N_A - N_B| \quad (2)$$

where S^{π}_{VB} stands for the ground-state spin quantum number of the π system of an alternant hydrocarbon and N_A and N_B are the numbers of the starred and unstarred carbon atoms in the hydrocarbons, respectively. It should be noted that the ground-state spins predicted by these two theories do not necessarily agree with each other, since their approaches are the limiting cases of MO and VB pictures, respectively. In fact, molecule **2**, which is the π-topological isomer of molecule **1**, is the first case that disclosed the disagreement between the two approaches.[7] This molecule itself is important for checking the validity of the above-mentioned spin-prediction theories by comparison with its π-topological isomer **2**. For molecule **2**, we obtain $S^{\pi}_{MO} = 1$ from eq 1 while $S^{\pi}_{VB} = 0$ from eq 2. Our experimental evidence shows that the VB approach is valid as far as the spin prediction for the ground state is concerned.[7,9,17] On the other hand, for molecule **1** both spin-prediction theories for the ground state agree with each other, giving $S^{\pi}_{MO} = S^{\pi}_{VB} = 1$. Thus we can expect a high-spin ground state for **1** in which the unpaired π spins in the π-NBMOs become parallel to each other. In molecule **1**, the other two unpaired electrons remain in the two nonbonding "n" orbitals localized at the divalent carbon atoms. These "n" spins are expected to be parallel via the ferromagnetic-exchange coupling to the unpaired π spins, since the "n" and π orbitals are mutually orthogonal at the divalent carbon atoms. As a result, both of the guiding principles predict a ground-state quintet ($S = 2$) for molecule **1**.

A remarkable change in the ground-state spin multiplicity has been found depending on the topology of their π electron networks. In this paper, we have described the results obtained by electron spin resonance (ESR) studies and by an unrestricted Hartree–Fock calculation using a generalized Hubbard model.[4d,32] Aims of this work are to illustrate the dependence of the ground-state spin multiplicity on the π electron network and to demonstrate the important role of the π topology in the spin alignment in organic molecules.

II. Experimental Section

A. Materials. The diazo precursor of **1**, 3,4′-bis(phenyldiazomethyl)biphenyl, **3**, was synthesized according to Scheme 1. Melting points were determined on a micro hot-state and are uncorrected. IR spectra were taken on a JASCO A-102 IR spectrophotometer. ^{1}H (100 MHz) and ^{13}C NMR (25 MHz) spectra were recorded on a JEOL FX-100 instrument. Only new compounds are described below.

3,4′-Dibenzoylbiphenyl. A mixture of 9.6 g (0.04 mol) of biphenyl-3,4′-dicarboxylic acid[33] and 34 mL of thionyl chloride was heated to a gentle reflux for 5 h under exclusion of moisture. The excess thionyl chloride was distilled off. The bis(acid chloride) was obtained as a light brown residue and used without purification for the following reaction. A solution of the bis(acid chloride) in 100 mL of dry benzene was added dropwise at room temperature to a suspension of 12.0 g of anhydrous aluminum chloride in 200 mL of dry benzene. The mixture was boiled with stirring for 3 h. Then the mixture was poured onto ice–water containing hydrochloride acid and the organic layer was separated. The remaining solid was dissolved in chloroform. The two organic solutions were washed separately with water and aqueous sodium hydroxide and dried over sodium sulfate. The crystals obtained after evaporation of the solvents were combined and recrystallized from ethanol to give 11.2 g (81%) of colorless prisms: mp 110–111 °C; IR (Nujol) ν_{CO} 1650 cm^{-1}; ^{13}C NMR ($CDCl_3$) δ 136.5, 137.1, 137.3, 138.1, 140.0, 144.0 (quarternary carbons), 196.4, 196.7 (carbonyl carbons). Anal. Calcd for $C_{26}H_{18}O_2$: C, 86.17; H, 5.01. Found: C, 85.98; H, 5.05.

3,4′-Dibenzoylbiphenyl Dihydrazone. A mixture of 3.6 g (0.01 mol) of the diketone and 25 mL of hydrazine hydrate in 150 mL of ethanol was heated under reflux for 24 h. The solvent was evaporated, and the residue was chromatographed on silica gel using benzene–ethyl acetate (5:1), giving 3.3 g (85%) of powdered hydrazone: IR (Nujol) 3340, 3250, 3190 cm^{-1}; ^{1}H NMR ($CDCl_3$) δ 5.41 (br s, 4H, exchangeable with D_2O), 7.18–7.80 (m, 18H, aromatic).

3,4′-Bis(phenyldiazomethyl)biphenyl (3). To a stirred solution of the dihydrazone (1.05 g, 2.7 mmol) in 100 mL of dry dichloromethane were added at 0 °C 2.8 g of active manganese dioxide (freshly prepared by Attenburrow's method[34]) and a few drops of saturated ethanolic potassium hydroxide in the dark. The reaction was monitored by measuring the growth of the IR absorption at 2040 cm^{-1} due to the diazo group of the aliquots. The absorbance became maximum at 2 h, after which the mixture was filtered. The wine-red solution was concentrated to a few milliliters under reduced pressure. Purple crystals

(21) Huber, R. A.; Schwoerer, M.; Benk, H.; Sixl, H. *Chem. Phys. Lett.* **1981**, *78*, 416.
(22) Seeger, D. E.; Lahti, P. M.; Rossi, A. R.; Berson, J. A. *J. Am. Chem. Soc.* **1986**, *108*, 1251–1265.
(23) Sugawara, T.; Tukada, A.; Izuoka, A.; Iwamura, H. *J. Am. Chem. Soc.* **1986**, *108*, 4272–4278.
(24) Izuoka, A.; Murata, S.; Sugawara, T.; Iwamura, H. *J. Am. Chem. Soc.* **1987**, *109*, 2631–2639.
(25) Dormann, E.; Nowak, M. J.; Williams, K. A.; Angus, R. O., Jr.; Wudl, F. *J. Am. Chem. Soc.* **1987**, *109*, 2594–2599.
(26) Chiang, L. Y.; Johnson, D. C.; Goshorn, D. P.; Bloch, A. N. *J. Am. Chem. Soc.* **1989**, *91*, 2743.
(27) Novak, J. A.; Jain, R.; Dougherty, D. A. *J. Am. Chem. Soc.* **1989**, *111*, 7618–7619.
(28) Rajca, A. *J. Am. Chem. Soc.* **1990**, *112*, 5889–5890. Rajca, A. *J. Am. Chem. Soc.* **1990**, *112*, 5890–5892. Rajca, A.; Utamapanya, S.; Xu, J. *J. Am. Chem. Soc.* **1991**, *113*, 9235–9241. Utamapanya, S.; Rajca, A. *J. Am. Chem. Soc.* **1991**, *113*, 9242–9251. Rajca, A.; Utamapanya, S.; Thayumanavan, S. *J. Am. Chem. Soc.* **1992**, *114*, 1884–1885.
(29) Veciana, J.; Rovira, C.; Crespo, M. I.; Armet, O.; Domingo, V. M.; Palacia, F. *J. Am. Chem. Soc.* **1991**, *113*, 2552–2561.
(30) (a) Minato, M.; Lahti, P. M. *J. Phys. Org. Chem.* **1991**, *5*, 459. (b) Minato, M.; Lahti, P. M.; van Willigen, H. *J. Am. Chem. Soc.* **1993**, *115*, 4532–4539. (c) Rajca, A.; Utamapanya, S.; Smithhisler, D. J. *J. Org. Chem.* **1993**, *58*, 5650–5652.
(31) (a) Longuet-Higgins, H. C. *J. Chem. Phys.* **1950**, *18*, 265–274. (b) Referring to simple but useful spin-prediction theories, the disjoint/nondisjoint description has been developed for biradicals by Borden and Davidson and demonstrated experimentally for a high-spin molecule by us. See ref 7 and Borden, W. T.; Davidson, E. R. *J. Am. Chem. Soc.* **1977**, *99*, 4587–4594.
(32) (a) Hubbard, J. *Proc. R. Soc.* **1963**, *276A*, 238–257. (b) White, R. M. *Quantum theory of magnetism*; Springer: New York, 1983; p 139.
(33) Woods, G. F.; Van Artsdale, A. L.; Reed, F. T. *J. Am. Chem. Soc.* **1950**, *72*, 3221–3226.
(34) Attenburrow, J.; Cameron, A. F. B.; Chapman, J. H.; Evans, R. M.; Hems, B. A.; Jansen, A. B. A.; Walker, T. *J. Chem. Soc.* **1952**, 1094.

were precipitated by addition of pentane: 850 mg (81%); mp 103–105 °C dec; IR (Nujol) ν_{NN} 2040 cm^{-1}. Anal. Calcd for $C_{26}H_{18}N_4$: C, 80.81; H, 4.69; N, 14.50. Found: C, 80.37; H, 4.32; N, 14.25.

B. ESR Measurements. Molecule **1** was generated at 4.2 K by the photolysis of 3,4′-bis(phenyldiazomethyl)biphenyl, **3**, oriented in a host single crystal of benzophenone ($P2_12_12_1$ space group with $Z = 4$[35]). The photolysis was carried out by 405 nm light from a 500 W high-pressure mercury lamp (OSRAM) equipped with a glass filter (TOSHIBA VY39) and a $CuSO_4$ solution filter (100 g of $CuSO_4{\cdot}5H_2O$/L, 5 cm light-path length). The mixed crystals were grown by slowly cooling in the dark a benzene–ethanol (1:1) solution containing a 0.028 mole fraction of **3** in benzophenone.

The polycrystalline powder used in the powder-pattern ESR measurements was obtained by pulverizing the mixed single crystals. The powder-pattern ESR measurements were carried out at 2.0 and 10 K with a Bruker ESP 300 spectrometer operating at the X-band equipped with a Bruker TE_{102} rectangular cavity ($Q = 6000$). The sample temperature was controlled with an Oxford ESR910 variable temperature controller.

Single-crystal ESR spectra were measured on a homemade spectrometer equipped with a JEOL K-band microwave (JES-SK) unit, a lock-in amplifier (PAR HR-8), a homemade cryostat, and a homemade TE_{011} cylindrical cavity ($Q = 12000$ at 4.2 K). In the single-crystal experiments, we adopted K-band frequency in order to accurately determine all the spin Hamiltonian parameters, especially the direction cosines of the principal axes of the fine-structure tensor in the crystallographic-axis system. The temperature dependence of the K-band ESR spectra was observed in the range from 4.2 to 250 K, where the sample temperature was measured with the Au–Cr thermocouple attached on the outside wall of the K-band cavity.

III. Analyses of ESR Spectra

To analyze the ESR spectra, we used the following spin Hamiltonian:[36]

$$\mathcal{H} = \beta\mathbf{B}\cdot\mathbf{g}\cdot\mathbf{S} + \mathbf{S}\cdot\mathbf{D}\cdot\mathbf{S}$$
$$= \beta\mathbf{B}\cdot\mathbf{g}\cdot\mathbf{S} + D[S_Z^2 - S(S+1)/3] + E(S_X^2 - S_Y^2) \quad (3)$$

where each term is used in the usual meaning. In this effective spin Hamiltonian, we neglected the higher order fine-structure terms such as BS^3, S^4, etc., since these terms allowed group-theoretically[36] are usually small for organic high-spin molecules.[5a,8c] In the K-band experiment, the angular dependence of the resonance fields was analyzed using the third-order perturbation theory. The general expressions for resonance fields and relative transition probabilities have been given for an arbitrary spin in our previous paper.[11]

In the simulation of the powder-pattern X-band ESR spectra, we assumed the Gaussian function for the line shape function of a single transition and a constant line width for all the transitions with $\mathbf{B}_0$ perpendicular to $\mathbf{B}_1$. The g tensor was isotropic for molecule **1**. This finding reduces the region in the Euler angles required for the simulation to an eighth part of the sphere, i.e., $\theta = 0 \leftrightarrow \pi/2$ and $\phi = 0 \leftrightarrow \pi/2$. The Euler angles θ and ϕ were varied from 0 to $\pi/2$ at 0.25 and 1 degree intervals, respectively. In order to reproduce the observed whole spectrum including the low-field forbidden transitions, we have also carried out the simulation with the help of the eigenfield method.[38] The ESR resonance fields were directly calculated by solving the corresponding eigenfield equation. The transition probabilities were, however, evaluated by numerically diagonalizing the spin Hamiltonian energy matrix of eq 3, in which the calculated resonance eigenfield was given, since the accuracy of the eigenvectors obtained from the solution of the eigenfield equation was not sufficient. Since the resonance field is independent of the third Euler angle, ψ,[11] the above procedure practically saves the computing time for the simulation of powder-pattern high-spin ESR spectra.[39]

IV. Results

A. Powder-Pattern ESR Spectra Observed at the X-Band and Occurrence of Off-Axis Extra Lines. Molecule **1** formed at 4.2 K by photolysis gave a powder-pattern ESR spectrum at the X-band shown in Figure 1a. This ESR spectrum was observed at 10 K on warming the sample. Figure 1b is the simulated spectrum for Figure 1a. In the simulated spectrum, Figure 1b, small bumps are seen which are particularly prominent in the range of 0.3 to 0.35 T. These are artefact due to the computation based on a smaller number of orientations with the larger intervals of θ and ϕ (0.25° and 1.0°, respectively). The best fit spin Hamiltonian parameters were found to be $S = 2$ (quintet spin state), $g = 2.003$ (isotropic), $|D| = 0.1250$ cm^{-1}, $|E| = 0.0065$ cm^{-1}, and the line width, $\Delta H_{msl} = 1.2$ mT. The microwave frequence employed was 9.5727 GHz. Figure 1c shows the angular dependence of the resonance fields for the Euler angles used to obtain the simulated spectrum. Since the agreement is excellent between the observed and simulated spectra, we can safely conclude that the observed ESR spectrum arises from the quintet electronic state. Figure 1c clearly indicates that the off-axis extra lines denoted by A in Figure 1b appear in addition to the normal stationary peaks denoted by X, Y, and Z which come from the three canonical orientations.[8b,11] One cannot expect any extra line to appear at the X-band in the case of the triplet spin multiplicity.[11] The off-axis extra lines are, therefore, key absorption peaks in the spin multiplicity assignment. The appearance of the extra lines assures that the observed spectrum arises from a quintet spin state. The extra lines shown in Figure 1 belong to the followng two cases:[11]

(I) $\theta \neq 0$, $\theta \neq \pi/2$, and $\phi = 0$

$$\cos(2\theta_{ex}) = [3(2M_S + 1)h\nu + 2(D - 3E)Q_{SM_S}]/[2(Q_{SM_S} - P_{SM_S})(D + E)] \quad (4)$$

(II) $\theta \neq 0$, $\theta \neq \pi/2$, and $\phi = \pi/2$

$$\cos(2\theta_{ex}) = [3(2M_S + 1)h\nu + 2(D + 3E)Q_{SM_S}]/[2(Q_{SM_S} - P_{SM_S})(D - E)] \quad (5)$$

for the transition $M_S \leftrightarrow M_S + 1$, where

$$P_{SM_S} = [4S(S+1) - 24M_S(M_S+1) - 9]/2 \quad (6)$$

and

$$Q_{SM_S} = -[2S(S+1) - 64M_S(M_S+1) - 3]/8 \quad (7)$$

From these equations we can calculate the Euler angle θ_{ex} where the extra stationary point of the resonance field appears. In the case of the quintet spectra shown in Figure 1, we obtained $\theta_{ex} = 26°$ (case I) and 29° (case II) for the transition $M_S = -1$

(35) Fleisher, E. B.; Sung, N.; Hawkinson, S. *J. Phys. Chem.* **1968**, *72*, 4311–4312.

(36) Abragam, A.; Bleaney, B. *Electron Paramagnetic Resonance of Transition Metals*; Clarendon Press: Oxford, 1970; p 341.

(37) Hutchison, C. A., Jr.; Kohler, B. E. *J. Chem. Phys.* **1969**, *51*, 3327–3335.

(38) Belford, G. G.; Belford, R. L.; Burkhalter, J. F. *J. Magn. Reson.* **1973**, *11*, 251–262.

(39) The simulation programs were made by one of the authors (Y.T.).

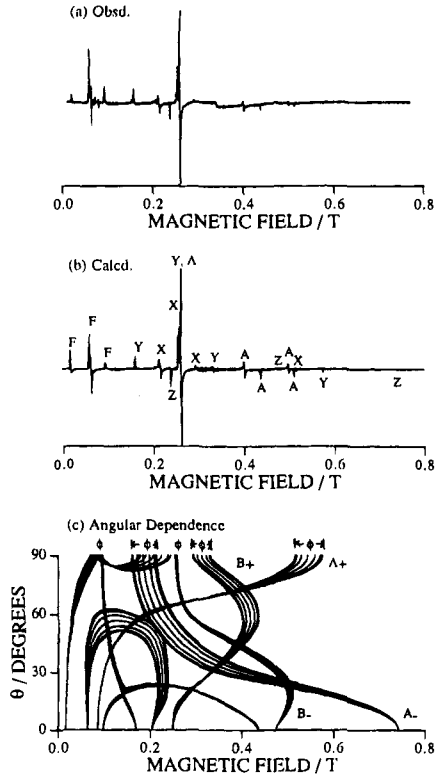

Figure 1. ESR spectra of the quintet molecule **1** in the polycrystalline powder observed at the X-band. The photolysis was carried out at 2 K. (a) The observed spectrum at 10 K. (b) The simulated spectrum. (c) The calculated angular dependence of the resonsance field, where $A_{\pm}$ and $B_{\pm}$ refer to the allowed transitions attributed to $M_S = \pm 2 \leftrightarrow \pm 1$ and $\pm 1 \leftrightarrow 0$, respectively, in the high-field limit. The angular anomaly giving the off-axis extra lines is denoted by A in (b).

$\leftrightarrow$ 0, and $\theta_{ex} = 54°$ (cases I and II) for the transition $M_S = 0 \leftrightarrow 1$, respectively, by substituting the observed D and E values and the microwave frequency employed into eqs 4−7. The angular dependence calculated by the eigenfield method shows the stationary points close to these angles' θ_{ex}'s as shown in Figure 1c.

Although the extra lines complicate the observed spectra, they are useful for the determination of the spin multiplicity. The analysis of the extra lines described above confirmed the assignment of the spin multiplicity, showing unequivocally that the ESR spectra of molecule **1** are attributable to the quintet spin state.

B. Single-Crystal ESR Spectra Observed at the K-band. To confirm the spin Hamiltonian parameters obtained in this experiment and to obtain the direction cosines of the principal axes of the fine-structure tensors, we made the following K-band measurements. Figures 2a and 2b show the two typical K-band ESR spectra of **1** observed at 4.2 and 77 K after the photolysis at 4.2 K, respectively. We have recorded the spectra in the dispersion mode in order to avoid saturation and to gain high sensitivity. The magnetic field was applied parallel to the crystallographic b axis of a host single crystal of benzophenone. A difference in the relative transition intensity between the spectra at 4.2 and 77 K was observed but the spectra were completely reversible for the temperature dependence. The difference could well be interpreted as originating in the difference of the Boltzmann population among the M_S sublevels. These spectra consist of two well-resolved pairs, $A_{\pm}$ and $B_{\pm}$. The relative separations of each pair are nearly $(A_- - A_+):(B_- - B_+) = 3:1$ and the relative integrated intensities of the transitions observed at 77 K are nearly $A_{\pm}:B_{\pm} = 2:3$. These ratios are

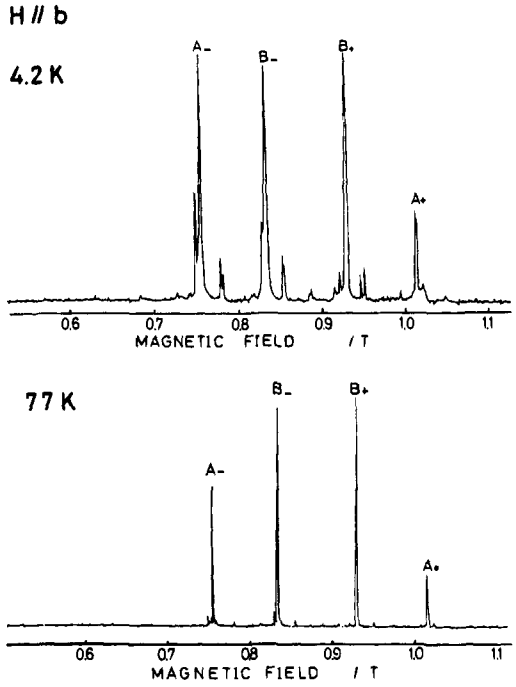

Figure 2. K-Band ESR spectra observed after photolysis at 4.2 K with the external magnetic field along the crystallographic b axis. (a) Observed at 4.2 K, the microwave frequency ν is 25062.3 MHz. (b) Observed at 77 K, $\nu = 25105.3$ MHz.

just what one expects for the $\Delta M_S \cong \pm 1$ allowed transitions between the M_S sublevels of the quintet ($S = 2$) spin manifold in the high field limit. The angular dependence of the resonance fields of the spectra in Figure 2b observed at 77 K is shown in Figure 3 with $\mathbf{B}_0$ applied in the crystallographic ab plane. The resonance fields, the signal intensities, and their angular dependence of the observed spectra were described well by the third-order perturbation calculation based on the effective spin Hamiltonian (3) with $S = 2$.[11] The g value, the fine-structure parameters, and the direction cosines of the principal axes of the fine-structure tensor were accurately determined by the least-squares method and they are listed in Table 1. They agree with those obtained by the powder experiment at the X-band within an experimental error. The error estimated for the D and E values is ca. $\pm 9 \times 10^{-4}$ cm^{-1} in the single-crystal experiment. The total error of the angles in determining the direction cosines with respect to the crystallographic axes was estimated to be within 1.5°. The energy level diagram, calculated by the exact numerical diagonalization of the spin Hamiltonian (3), is shown in Figure 4, which corresponds to the same orientation of the magnetic field as in Figure 2. The absolute sign of the D value was determined to be positive from the effect of the Boltzmann distribution as shown in Figures 2a and 2b, which can be calculated using the energy level, illustrating that K-band experiments simplify the determination of the absolute sign of D because of the higher transition energy than in X-band. The ESR spectra shown in Figure 1 were unchanged from 4.2 to 250 K, except for the change in the relative intensities according to the Boltzmann population, and no other spectra appeared. This finding indicates that the other spin states can be located at higher than 300 cm^{-1} above the ground state. Thus, we can conclude the observed quintet state to be the electronic ground state.

V. Discussion

A. Spin Alignment of 3,4′-Bis(phenylmethylene)biphenyl. It is known that molecule **2**, which is a π-topological isomer of

1, has the ground-state singlet with a closely located triplet and quintet state.[7,17] On the other hand, this work shows that molecule **1** has the high-spin ground state with other low-spin states located far above it, illustrating that a change in the ground-state spin depends on the topology of the π electron network. In order to give rationale for this finding, we have adopted a more sophisticated UHF theoretical calculation of the electronic structure of **1**.

The two approaches as mentioned earlier in this paper are both the limiting case of MO and VB theory, respectively. There has been no other tractable method[31b] that enables us to treat spin-polarized large quantum systems such as organic high-spin molecules and to give us reasonable physical pictures for their spin density distributions. In particular, the simple MO approach does not allow us to explicitly treat spin correlation or the nature of spin polarization of the systems. We have been focusing our attention on the nature of the spin polarization from both experimental and theoretical sides.[9,10,14,17,18] Theoretically, we have introduced a generalized Hubbard Hamiltonian approach as a tractable method for elucidating electronic structures of spin-polarized large molecular systems.[9] The method is semiempirical because we determine Hamiltonian parameters (U/T and J/T) empirically, but it is applicable to large organic systems with both n and π spins, providing quantitatively their spin density distributions in the ground state.

To better understand the spin alignment in molecule **1**, we have carried out a semiempirical UHF calculation of its electronic structure using the generalized Hubbard Hamiltonian,[4d,32]

$$\mathcal{H} = -T \sum_{m,m',\sigma} a^{+}_{m',\sigma} a_{m\sigma} + (U/2) \sum_{m,\sigma} n_{m-\sigma} n_{m\sigma} - J \sum_{k} [S^{Z}_{k} S^{Z}_{m} + (S^{+}_{k} S^{-}_{m} + S^{-}_{k} S^{+}_{m})/2] \quad (8)$$

where a^{+} and a are the creation and annihilation operators, respectively, and $n_{m\sigma} = a^{+}_{m\sigma} a_{m\sigma}$. The subscripts m and k refer to the π and n carbon sites. T is a π-electron transfer integral (i.e., minus Hückel β) between the adjacent carbon sites. U and J are the effective on-site Coulomb repulsion between the two π electrons and the exchange integral between the n and π electrons at the divalent carbon atoms, respectively. It should be noted that in our previous work[17] the values for U/T and J/T were taken as 1.0 and 0.25, respectively, but in this calculation we have adopted $U/T = 2.0$ and $J/T = 0.25$ as a more appropriate set of the parameters. It turns out that the latter set gives more satisfactory agreement between the observed and calculated π spin densities of a series of high-spin carbene oligomers such as 1,3-bis(phenylmethylene)benzene. We have solved this model Hamiltonian by employing the Hartree–Fock approximation,

$$n_{m\sigma} n_{m-\sigma} = \langle n_{m\sigma} \rangle n_{m-\sigma} + \langle n_{m-\sigma} \rangle n_{m\sigma} - \langle n_{m\sigma} \rangle \langle n_{m-\sigma} \rangle \quad (9)$$

where $\langle\ \rangle$ denotes the average with respect to the spin state in question. The total spin is not generally conserved in the UHF calculation. This is not so significant for high-spin ground states because of the small amount of the spin contamination for the present case. As the result of this calculation, the quintet spin state was the most stable electronic spin state for molecule **1**. Figure 5 shows the calculated spin density distribution in the quintet ground state. On the basis of this spin distribution, we can understand the spin alignment of **1** as follows. The unpaired π spins are distributed over the carbon skeleton by alternating the sign of the spin density from carbon to carbon, thus leading to the formation of the pseudo spin density wave in the π electron network (pseudo π-SDW). The localized n spins in the σ dangling bonds are exchange-coupled ferromagnetically ($J > 0$ in eq 8) to the unpaired π spins at each divalent carbon atom, causing the n and π spins to be parallel to each other. Since molecule **1** has the same sign of the π spin density at both divalent carbon atoms as a result of the pseudo π-SDW, this molecule has four parallel spins, leading to the quintet ground state, because the π-SDW situation is most favorable in view of the total spin exchange-correlation energy. The formation of the pseudo π-SDW state depends strongly on the topology of the π electron network, i.e., the first term of the Hubbard Hamiltonian (8), which indicates the important role of the π topology also demonstrated in this work. The physical picture of the spin alignment of **1** obtained by the Hubbard calculation has been confirmed in terms of the spin density distribution determined by our ENDOR experiments. The results will be published elsewhere.[18]

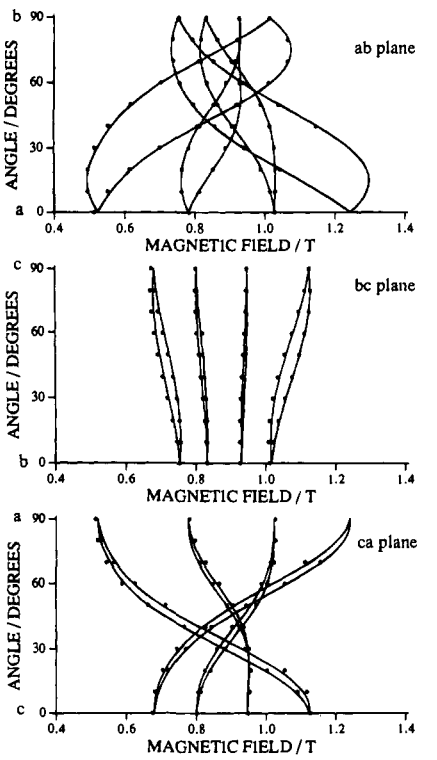

Figure 3. Angular dependence of the K-band resonance fields of the allowed transitions observed at 77 K for rotation of the magnetic field in the crystallographic *ab* plane ($\nu = 25105.3$ MHz). The solid points represent the observed values and the solid curves the calculated ones by the third-order perturbation theory.[11] The primed pair $A'_{\pm}$, $B'_{\pm}$ and the unprimed pair $A_{\pm}$, $B_{\pm}$ arise from the two magnetically nonequivalent sites occupied by **1** in the benzophenone host crystal.

B. Probable Molecular Conformation of 1. The knowledge of the principal axes of the fine-structure tensor provides valuable information about the molecular conformation of **1** in the host benzophenone single crystal, as described below. The fine-structure tensor of **1** can be calculated semiempirically by the expression[8c]

$$D_{ij} = [S(2S-1)]^{-1} (\varrho_k/\varrho_{DPM})(\mathbf{U}_k \cdot \mathbf{d}_{DPM} \cdot \mathbf{U}_k^{\dagger})_{ij}, \quad i,j = X,Y,Z \quad (10)$$

where $\mathbf{d}_{DPM}$ is the fine-structure tensor observed for diphenylmethylene ($S = 1$),[37] ϱ_k and ϱ_{DPM} are the π spin densities on the kth divalent carbon atom of **1** and on that of diphenylmethylene, respectively, and $\mathbf{U}_k$ is a unitary matrix which transforms the local symmetry axes for the divalent carbon

Table 1. Hamiltonian parameters g, D, and E and the Direction Cosines for the Principal Axes of the Fine-Structure Tensor

					direction cosines		
	g	D (cm^{-1})	E (cm^{-1})	principal values (cm^{-1})	a	b	c
quintet, $S = 2$	2.003	0.1256	−0.0058	X −0.0477	0.0140	−0.1951	0.9807
				Y −0.0360	−0.2594	0.9465	0.1920
				Z 0.0837	0.9657	0.2571	0.0374

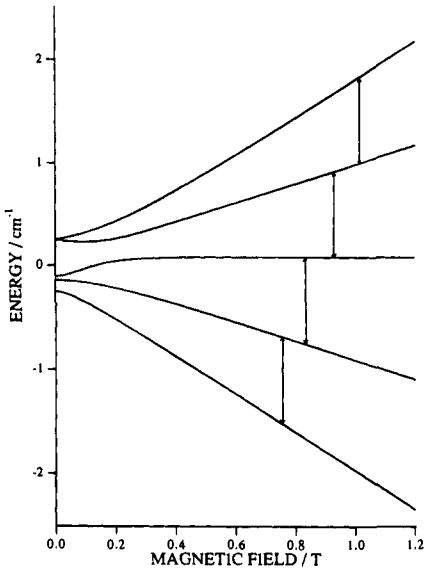

Figure 4. Energy level diagram of the Zeeman sublevels and transitions predicted for molecule **1** with the external magnetic field along the b axis.

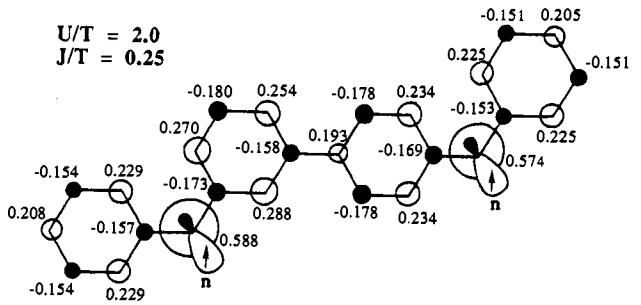

Figure 5. π-Spin density distribution of the quintet ground state ($S = 2$) of **1** obtained by a UHF calculation using a generalized Hubbard model.

moiety of **1** to the X, Y, Z axes referred to the molecular frame. This semiempirical formula was derived by assuming that the one-center n−π interaction predominantly contributes to the spin−spin interaction. These π spin densities were obtained by the UHF calculation using the Hubbard model Hamiltonian (8): $\varrho_{DPM} = 0.589$, while $\varrho_1 = 0.588$ and $\varrho_2 = 0.574$ as shown in Figure 5. For $\mathbf{d}_{DPM}$, the following observed values are used: $d_{DPM,XX} = -0.1542$, $d_{DPM,YY} = -0.1158$, and $d_{DPM,ZZ} = 0.2700$ cm^{-1}, respectively.[37] Molecule **1** can take four different conformations even when only a planar structure is assumed. These possible molecular conformations and their semiempirically calculated fine-structure parameters are given in Figure 6. The Z axis is nearly along the molecular long axis and the X axis is perpendicular to the molecular plane. The positive sign of the observed D value ruled out the possibility of conformation IV. On choosing the most probable conformation, we have also taken the consistency with the crystal structure into account. The most probable conformation was determined to be conformation I in Figure 6, whose projection onto the ab plane of the host crystal is shown in Figure 7. This figure shows

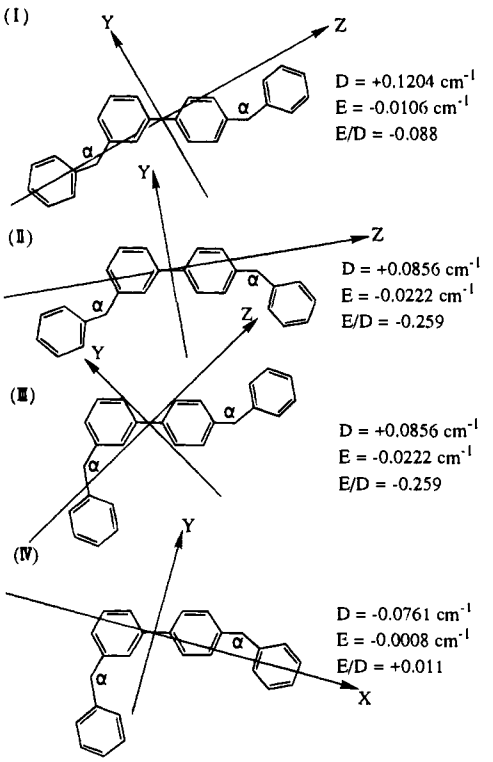

Figure 6. Probable molecular conformation of **1**. The fine-structure parameters D and E and the principal axes are those calculated for the bond angle of the divalent carbon atom, $\alpha = 150°$.

that this conformation requires the substitution of two sites of benzophenone over the two unit cells.

VI. Conclusions

We have investigated a novel high-spin carbene, **1**, both by powder-pattern and single-crystal ESR spectroscopies by the comparison of molecule **2**, which is a π-topological isomer of **1** and also known as the first example which violates the spin prediction[7] on the basis of a simple MO theory[31a] plus Hund's rule. The results obtained in this work can be summarized as follows: (1) It has been proven by analyses of ESR spectra that **1** is quintet ($S = 2$) in its electronic ground state. The calculation based on the spin Hamiltonian (3) with $S = 2$ has well reproduced the observed resonance fields and intensities. In contrast, the ground state of **2** is known to be singlet ($S = 0$) as already reported in our previous paper.[7,17] (2) The most important point is that a change in the spin multiplicity of the ground state has been illustrated, depending on the topology of the π electron network of alternant hydrocarbons. (3) The mechanism of the intramolecular spin alignment of **1** was interpreted by the UHF calculation using a generalized Hubbard Hamiltonian. The formation of the π-spin density wave (pseudo π-SDW) depending on the π topology was clarified, giving the physical picture of the spin alignment. (4) Finally, the observed fine-structure parameters were reproduced by the semiempirical calculation. The most probable molecular conformation in the host crystal was determined from the observed fine-structure tensor with the help of the semiempirical calculation.

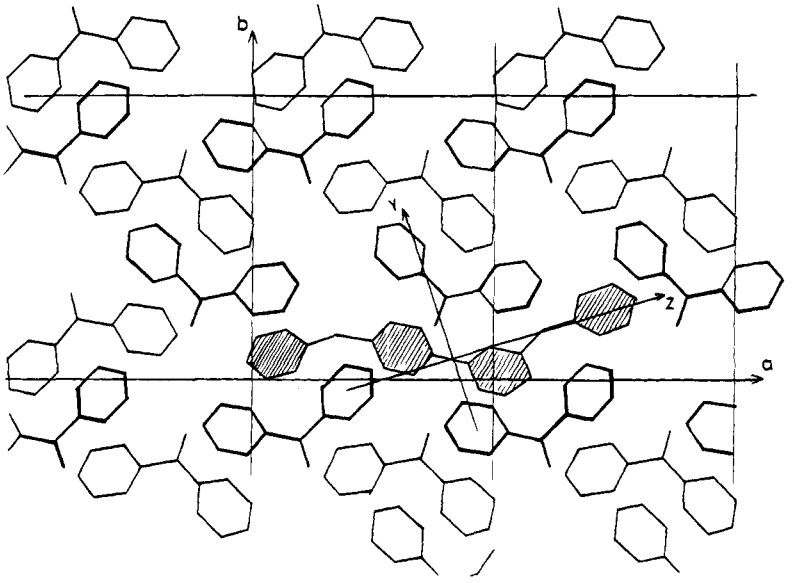

Figure 7. Crystal structure of benzophenone and the orientation of the conformation I (shaded) shown in Figure 6 in the crystal which is projected in the crystallographic *ab* plane. The molecules drawn with thin lines have their mid points at $z = 0$ and those with heavy lines at $z = 1/2$, where z is the height along the crystallographic c axis.

Scheme 1

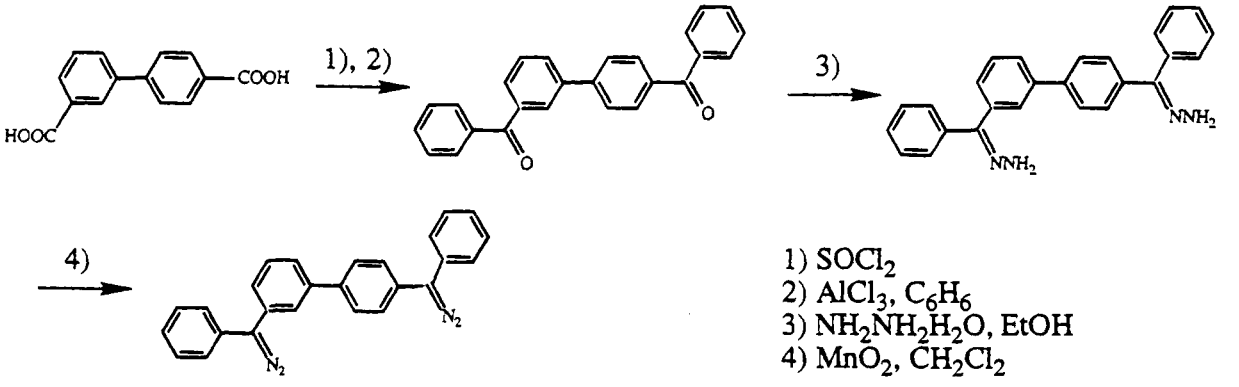

Acknowledgment. The present work was supported by a Grant-in-Aid for Scientific Research and for Priority Areas from the Ministry of Education, Science and Culture, Japan. The authors thank the Computer Center of the Institute for Molecular Science, Okazaki National Research Institutes, for the use of the HITAC M-680H.